Appl. Phys. B 88, 507–513 (2007)
DOI: 10.1007/s00340-007-2698-3

Applied Physics B
Lasers and Optics

R.J. HENDRICKS✉
D.M. GRANT
P.F. HERSKIND
A. DANTAN
M. DREWSEN

An all-optical ion-loading technique for scalable microtrap architectures

QUANTOP – Danish National Research Foundation Center for Quantum Optics,
Department of Physics and Astronomy, University of Århus, 8000 Århus C., Denmark

Received: 12 April 2007 / Revised version: 14 May 2007
Published online: 23 June 2007 •

ABSTRACT An experimental demonstration of a novel all-optical technique for loading ion traps, which has particular application to microtrap architectures, is presented. The technique is based on photoionisation of an atomic beam created by pulsed laser ablation of a calcium target, and provides improved temporal control compared to traditional trap loading methods. Ion loading rates as high as 125 ions per second have so far been observed. Also described are observations of trap loading where Rydberg state atoms are photoionised by the ion Doppler cooling laser.

PACS 32.80.Fb; 32.80.Dz; 39.10.+j; 52.38.Mf

1 Introduction

In recent years, a number of experiments have demonstrated ion traps to be a viable technology for quantum information processing (QIP) and direct quantum simulation [1–3]. There are, however, a number of obstacles that must still be overcome if ion trap QIP is to solve problems that are intractable using classical computing methods.

One of the most important of these obstacles is the scaling up of current experiments to enable processing of much larger numbers of ion qubits. As a result, there has been much recent interest in the development of microscale arrays of ion traps [4–7].

Besides the challenges involved in fabrication of microtrap arrays, there are a number of problems associated with reducing the size of ion traps. One of the most significant of these is the observation that the rate at which ions are heated has been measured to increase dramatically as the trap size is reduced. Experiments have measured the heating rate to vary with trap scale, r, as strongly as r^{-4} [8]. This increase is attributed to patch potentials due to the presence of contaminants on the trap electrodes. Often this contaminant material is deposited by the atom sources used to load ion traps [9]. An interesting observation is that the effect of these patch potentials can be significantly suppressed by cooling of the trap electrodes to cryogenic temperatures.

At present, most ion traps are loaded by electron bombardment or photoionisation of a neutral atomic beam [10]. Atoms are typically emitted from a resistively heated oven, and a series of skimmers is used to produce from this source a nominally collimated atom beam that is directed towards the centre of the trapping region. This beam is continuous and cannot be rapidly switched on or off, so many more atoms are sent through the trap than required. Over time this can lead to the build up of material on trap electrodes and nearby surfaces. A cleaner ion-loading technique would result in less build up of contaminant material on electrodes and therefore reduce the extent of heating as the trap size is reduced. An atom source that can be more rapidly turned on and off to provide a better controlled atom flux than a traditional thermal source is therefore highly desirable.

An interesting alternative that has recently been demonstrated is the loading of an ion trap by photoionising laser-cooled atoms in a MOT that overlaps the ion-trapping region [11]. Although technically demanding, this approach has the advantages of a very high loading efficiency and low ion temperatures.

Here we present a general all-optical technique for loading ion traps that has a number of advantages over thermal atom sources. In our experiment a pulsed laser source is used to ablate material from a calcium metal surface. The atoms produced are directed through the trap, where they are photoionised. Through rapid switching on and off of the ablation laser, atoms can be produced in brief pulses only when required [12]. This reduces the overall amount of material passing through the trap and so reduces electrode contamination. The pulsed nature of the technique also makes it suitable for the controlled production of single ions, as required for scalable QIP. The general technique can be scaled down in size in order to better integrate with microtrap structures, can be used with many different atomic species and is, in principle, compatible with operation at cryogenic temperatures.

2 Laser ablation

Laser ablation is a diverse and complex field and the reader is directed to references [13, 14] for an overview. In brief, there are two distinct regimes in which nanosecond pulse laser ablation occurs, distinguished largely by the laser fluence (energy deposited on a surface per unit area by each pulse). Here we are principally concerned with the low fluence regime, in which thermal processes are dominant. If the laser pulse duration is much shorter than the timescale for thermal conduction processes then the region of the target

✉ Fax: +45 8612 0740, E-mail: rjh@phys.au.dk

that is irradiated by the laser may be locally heated to high temperatures [15]. This can result in melting, sublimation or desorption of material in the affected region. Laser ablation in this thermal regime has previously been used to reduce the amount of source material required for resonance ionisation mass spectrometry [12]. The motivation is therefore similar to that described in the present work.

As the laser fluence is increased, multi-photon excitation will eventually lead to ionisation of material at or near the target surface, resulting in the formation of a plasma phase [16]. This can dramatically increase the rate at which energy is absorbed from the laser beam. In this high fluence regime there are a variety of mechanisms by which material can be ejected from the target surface, some of which occur on a macroscopic scale [13]. For the purposes of loading ion traps the plasma regime may sometimes be undesirable because a significant number of excited state atoms can be produced.

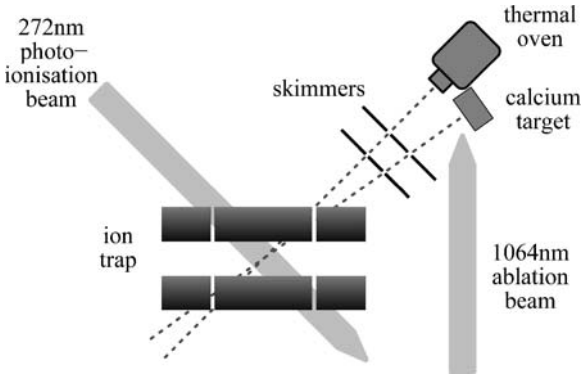

FIGURE 1 Ion-loading setup within the trap chamber. Atoms are produced either from a thermal source or from a calcium target irradiated with light from a pulsed Nd:YAG laser. A series of skimmers prevents any of this material from contaminating the trap electrodes. Atoms that reach the centre of the trap can be photoionised by 272 nm light directed almost perpendicular to the atomic beams

3 Experimental techniques

In our experimental setup we trap $^{40}Ca^{+}$ ions. These ions are laser cooled on the rapid $S_{1/2} \longrightarrow P_{1/2}$ dipole transition at 397 nm. A repumper at 866 nm is required in order to prevent build up of population in the metastable $D_{3/2}$ state [17]. Ions are detected by imaging the spontaneously re-emitted 397 nm light onto an image intensifier, the output of which is monitored with a CCD camera. The fluorescence rate on the 397 nm transition is such that, given the magnification in the optical system of approximately 10, it is possible to detect and resolve individual ions.

The ion trap used in these test experiments is a linear radiofrequency trap that has been described in detail elsewhere [18]. It has a trap size parameter, r, of 2.35 mm and is operated at a frequency of 4.0 MHz. In order to reduce the rate of collisions between the ions and background gas particles, the trap is housed in an ultra-high vacuum chamber at a base pressure of approximately 4×10^{-10} mbar, as measured on an ion gauge within the chamber.

With appropriate trapping voltages it is possible to form linear strings of ions or Coulomb crystals containing rather large numbers of ions [19, 20]. The number of ions in such crystals can be determined by measuring the overall crystal volume and using the trapping parameters to calculate the ion density [20, 21].

Usually the trap is loaded using atoms from a thermal source (described in [10, 18]). A series of skimmers is used to trim the distribution of emitted atoms into a narrow beam, which is approximately 1.0×1.5 mm at the centre of the trap (see Fig. 1). The thermal source is about 13 cm from the trap, so a rather small fraction of the atoms produced passes through the skimmers. Atoms passing through the centre of the trap can be photoionised in a two-photon process by light at 272 nm. The first step in this process is a resonant transition and hence it is isotope selective. The relevant energy levels are shown in Fig. 8 and full details can be found in [10, 17]. The 272 nm light is generated by frequency-quadrupling light from a fibre laser at 1088 nm [22]. Typically, the 272 nm power used is about 15 mW, and the beam waist at the centre of the trap is approximately 160 μm. In order to reduce Doppler shifting of the ionisation laser frequency due to the velocity of the atoms in the beam, the propagation direction of the laser is chosen to be perpendicular to that of the atom beam.

In the present work, a pure calcium metal target is placed close to the thermal source with an identical set of skimmers leading to the centre of the trap (see Fig. 1). The surface of the calcium target is aligned such that it is perpendicular to the path towards the trap centre. Due to geometric constraints, this path is aligned at an angle of about 12° relative to the ionisation laser.

The ablation laser used in these experiments is a 1064 nm pulsed Nd:YAG laser (CrystaLaser QIR-1064-500). The maximum pulse energy is about 80 μJ and remains constant for pulse repetition rates up to about 3 kHz. At repetition rates higher than this the maximum energy begins to decline, and by about 15 kHz it falls as the inverse of the repetition rate. Pulse durations are also dependent on the repetition rate, but are in the region of 30–50 ns for the rates used here. The maximum repetition rate is 200 kHz. The laser is focussed onto the calcium target with a waist of about 75 ± 15 μm. In our current setup we are restricted to using an angle between the laser propagation direction and the normal to the calcium surface of approximately 30°. This means that the region illuminated by the ablation laser will be slightly larger in one direction than the measured beam waist.

Alignment of the ablation laser is performed by imaging the target with a CCD camera directed parallel to the beam path (see Fig. 2). With a low pulse energy but large repetition rate, scattered light from the calcium target is clearly visible and allows positioning of the beam. By placing a filter in front of the CCD camera, this light at 1064 nm is eliminated. The pulse energy can then be gradually increased until light from the calcium target is once again seen on the camera. This light at a wavelength other than 1064 nm is a clear indication of the generation of plasma on the calcium surface. The focussing of the ablation laser beam can then be optimised by finding the point at which plasma is observed with the lowest pulse energy. Once the position of focus has been optimised, we find that plasma can be clearly seen with ablation laser fluences above about 600 mJ/cm^2.

To ensure that the ablation beam covers the region of the calcium target that is aligned with the skimmers and the centre

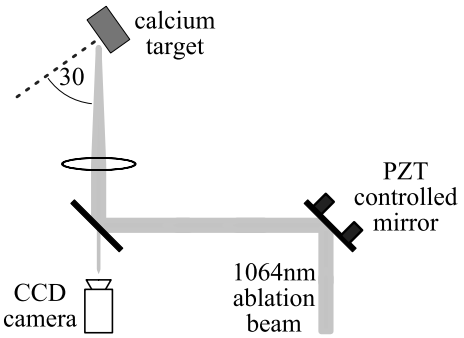

FIGURE 2 Setup for alignment and control of the ablation laser beam. The CCD camera images the target surface and is used for initial laser alignment. By filtering out light at 1064 nm it can also be used to monitor the extent of plasma formation at the target. The PZT controlled mirror is used to dither the beam position in the vertical and horizontal directions

of the trap, a PZT controlled mirror is used to dither the beam position over a region of about 1 mm^2. We have found that this also helps to keep the ablation rate stable.

In addition to the main ion trap setup, we have also constructed a simple test chamber for characterising the ablation process. In this chamber we can use larger targets and can rapidly replace them after use. This means that we can ablate much larger quantities of material and can use targets with a much greater visible surface area, so that we can ablate many holes using different laser parameters. The test chamber is pumped down to a pressure of about 1×10^{-5} mbar. The alignment procedure and beam dithering technique are the same as those used in the ion trap setup described earlier. In this setup the ablation laser waist is approximately 55 ± 15 μm and the propagation direction is almost normal to the calcium surface. Due to uncertainties in beam waist measurements and the rather different angles of incidence, care should be taken when comparing fluence measurements in the two setups.

To determine the quantity of material that has been ablated from the target in this setup, we remove the target and use optical microscopy to measure the dimensions of the ablation craters. For this technique to be effective we must necessarily remove material to a depth of at least a few micrometers.

4 Results

Using a calcium target in the test chamber, the ablation depth as a function of pulse energy has been studied using in each case 4.6 million pulses fired at a repetition rate of 2.4 kHz. The results are plotted in Fig. 3a. The bars in this plot indicate the maximum and minimum depth of the ablation hole relative to the original calcium surface. With fluences less than or equal to about 600 mJ/cm^2 there are regions that are actually raised relative to the initial surface and it is impossible to precisely determine how much material has been removed. What is seen using optical microscopy is a series of raised and pitted regions that seems to be due to localised melting and redistribution of the metal surface. This would be consistent with a very low ablation rate resulting from a thermally driven process. It would appear from Fig. 3a that there is a threshold fluence at which the ablation rate begins to increase much more steeply, and almost linearly with the laser

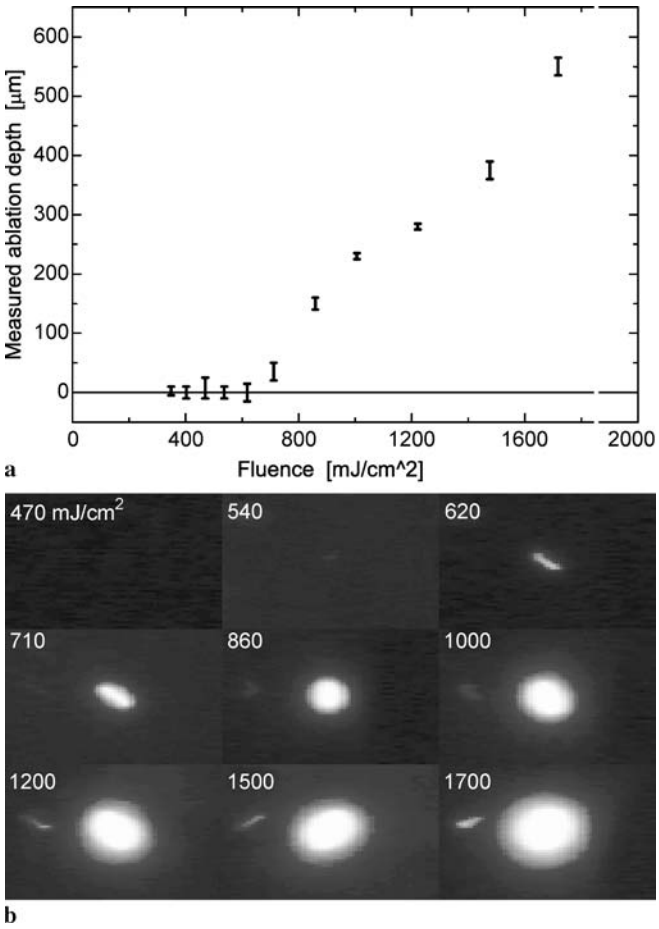

FIGURE 3 (**a**) Depth of holes ablated in a calcium target after 4.6 million pulses, plotted as a function of laser fluence. The *bars* indicate the measured maximum and minimum depth of the ablated surface, relative to the original surface. The observed threshold behaviour at about 600 mJ/cm^2 appears to correspond to the onset of plasma formation. (**b**) CCD images of the target showing the extent of the plasma for different ablation laser fluences (marked on the images in mJ/cm^2). Each image corresponds directly to a plotted point in (**a**). The images are single frames accumulated in 1/30th of a second. Thus each image integrates over several hundred ablation laser pulses

fluence. This would seem to correspond to the onset of plasma generation and hence the presence of a second, much more rapid, ablation mechanism. This is supported by the direct observation of plasma formation at around this fluence, using a CCD camera with strong filtering of the scattered light at 1064 nm. Typical images taken with this camera at different ablation laser fluences are indicated in Fig. 3b. The faint second image to the left of each plasma plume is due to double reflection in the beamsplitter placed in front of the CCD camera.

It is important that atoms are emitted in their electronic ground states if the photoionisation process is to remain isotope-selective. In practice this means that ablation must be carried out in the thermal regime, where plasma effects are not observed. Note also that given the extremely small atom flux required for loading an ion trap, it is anticipated that the lifetime of a calcium target can be very long.

In the ion trap setup, ions can be loaded into the trap by irradiating the calcium target with the ablation beam whilst the photoionising laser is operating continuously. Figure 4 shows

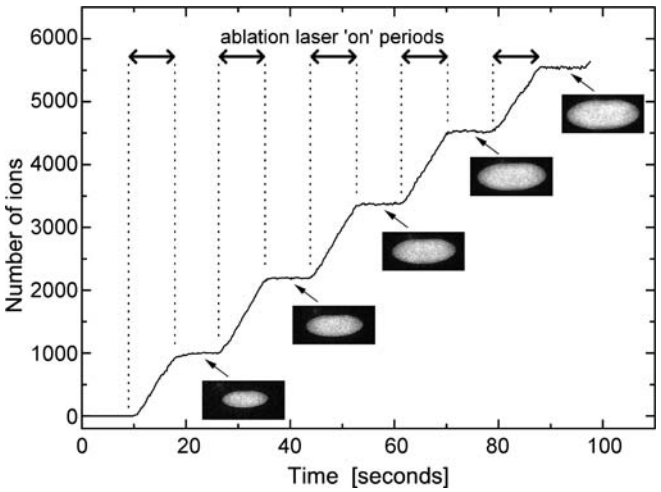

FIGURE 4 Number of ions present in the trap as a function of time, when the ablation laser is periodically gated on and off. The ion number is seen to increase only during the 'on' phase of the gating cycle, indicated by the double-headed *arrows*. The ion number is determined from analysis of the dimensions of the ion crystal in the trap at each point. The *inset* images are examples that show the state of the crystal at the indicated times. The ablation laser fluence used is 240 mJ/cm^2 and the repetition rate is 25 kHz

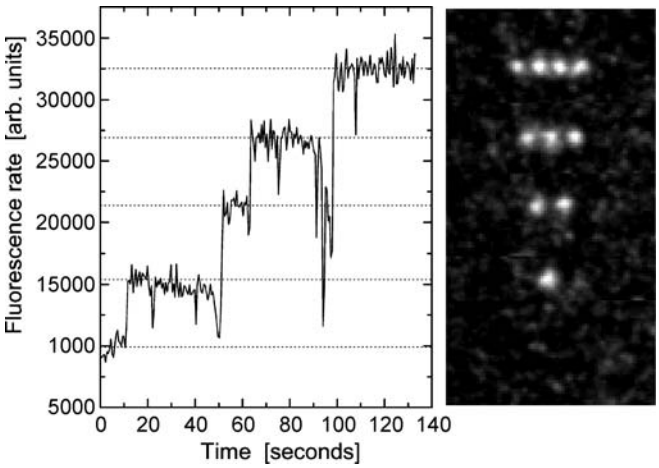

FIGURE 5 Fluorescence detected from the centre of the trap as a function of time during continuous ablation with a laser fluence of 120 mJ/cm^2 and repetition rate of 50 kHz. With these parameters the loading rate is extremely small and single ions can easily be loaded. The intensified CCD images show the ion string shortly after each ion is loaded

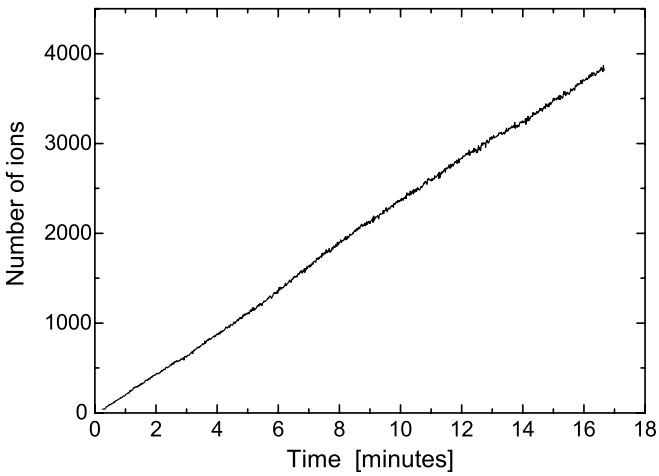

FIGURE 6 Number of ions present in the trap as a function of time during continuous ablation with a fluence of 240 mJ/cm^2 and repetition rate of 25 kHz. The photoionisation parameters are set such that the loading rate observed is rather small, but it is seen to be almost constant for a period of more than 15 minutes

the calculated number of ions present in the trap as a function of time, whilst the ablation laser is periodically gated with regular 'on' and 'off' periods of nine seconds. The number of ions is seen to increase during the 'on' periods. This increase stops abruptly whenever the laser is switched off, indicating that ion loading is indeed due to ionisation of calcium atoms emitted by the ablation process.

The loading rate is found to be dependent on the ablation laser fluence. Rates as high as 125 ions per second have been observed so far, using a fluence of 240 mJ/cm^2 at a repetition rate of 25 kHz. There are many other parameters that can affect the loading rate, such as the ablation beam positioning and the photoionisation laser wavelength and intensity. It is expected that with further optimisation even greater loading rates may be achieved, whilst still keeping the ablation laser fluence well below that required to generate plasma.

In order to demonstrate the ability of the ablation loading technique to load individual ions in a controlled manner, experiments have been carried out with laser fluences as low as 120 mJ/cm^2. In this regime ions are loaded rather slowly, and it is a straightforward task to shutter the ablation laser once a desired number of ions is reached. Figure 5 shows a number of frames taken from a series of CCD images recorded during continuous ion loading at this laser fluence. The number of ions present in the string is clearly apparent in each frame. Also shown in Fig. 5 is the overall fluorescence as determined by integrating the signal in a fixed area of each of the CCD images. The time at which each of the ions is loaded is clearly marked by a discrete step in the fluorescence level. Brief drops in fluorescence are sometimes observed shortly before a new ion is observed. These drops are due to heating of the ions already in the trap by the new, much hotter ion. Drops in signal are sometimes seen at other times, when an ion is excited into a non-fluorescing state through collisions with atoms passing through the trapping region.

Although the rate at which ions are loaded in this example is intentionally rather small, it would be relatively straightforward to implement a loading scheme in which the fluorescence rate is continually monitored and the ablation laser is automatically shuttered when an ion is loaded. With such a system, individual ions could be controllably loaded at higher fluences and hence much more rapidly.

In order to achieve well controlled loading of the trap, it is important that the loading rate be stable over time. That this is the case is demonstrated in Fig. 6, which shows the number of ions in an ion crystal during more than 15 minutes of continual loading. The very slight oscillation in the loading rate can probably be attributed to drift in the wavelength of the photoionising laser, since similar effects are seen during loading with a thermal source.

An additional benefit of the laser ablation-based ion-loading technique is that the pressure rise during loading can be kept relatively small. Thermal atom sources must necessar-

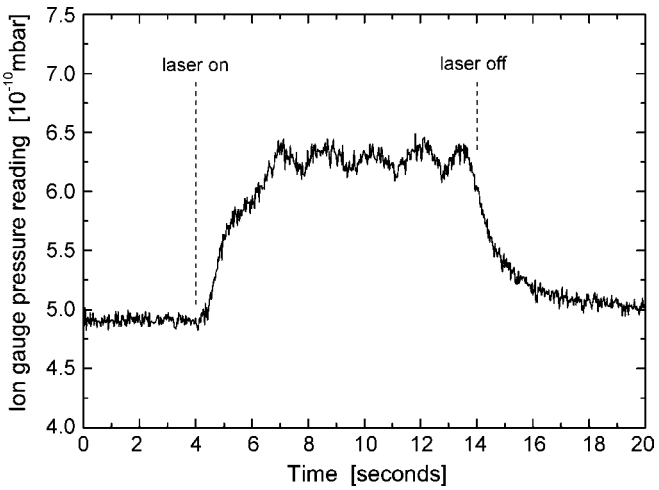

FIGURE 7 Response of ion gauge pressure measurement to a ten second period of ablation loading with a laser fluence of 270 mJ/cm^2 and repetition rate of 23 kHz. An increase in the equilibrium pressure of about 1.5×10^{-10} mbar is observed. The pressure returns to its initial value within a few seconds of switching off the ablation laser

ily be maintained at some high temperature during operation. This raised temperature often leads to a significant increase in the background pressure within the vacuum chamber. Even after loading is completed it can take several minutes for the pressure to return to its initial level. During laser ablation, the surface area of the target that is strongly heated is governed by the size of the ablation beam. Since this can be very small, it is possible to avoid large pressure rises during loading and obtain much more rapid recovery times.

Upon first ablating the surface of the calcium target in our ion trap setup, the pressure was observed to rise as high as 10^{-8} mbar. This initial increase is ascribed to evaporation of contaminant material on the surface layer of the target. As ablation continued, much of this contaminant layer was removed and the pressure in the chamber improved.

The typical pressure response during ablation of the calcium target with a relatively large laser fluence of 270 mJ/cm^2 and a repetition rate of 23 kHz is shown in Fig. 7. The ablation continues for a period of ten seconds, during which the pressure rises to a new equilibrium level that is approximately 1.5×10^{-10} mbar greater than the base pressure. The pressure returns to its initial value within a few seconds of switching off the ablation laser. Although the pressure rise observed during ablation is actually comparable to that expected from a thermal source that has been used for some time, the situation might have been improved by stronger heating of the calcium target to remove contaminants. This could have been achieved by resistively heating the target during bakeout of the vacuum chamber. Even now it is possible that the pressure rise will be reduced over time as more contaminants are removed from the target surface.

5 Photoionisation of Rydberg atoms

Besides the trap loading technique described in the previous sections, we also observed that at relatively high ablation laser fluences ions can be loaded into the trap without the use of the photoionisation laser at 272 nm. The loading rates for this process can be as high as 25 ions per seconds. Although it is not fully understood how the various experimental parameters affect the loading rate we do find that at relatively low fluences it is possible to eliminate this loading process altogether. Indeed, during collection of all the data presented in the previous section no loading was observed without the 272 nm laser.

This loading of the trap without the 272 nm laser is surprising, especially since it occurs even if the 866 nm repumper laser is blocked. This eliminates the laser cooling force and makes it extremely unlikely that an ion generated outside the trap is captured. It follows that the ions must be generated near the centre of the trap as a result of photoionisation by the Doppler cooling or repumper lasers. By blocking each of these beams in turn, it has been determined that it is only the 397 nm cooling beam that is responsible for this photoionisation.

Since it takes some time for the ablated atoms to reach the centre of the trap, they must necessarily be produced in some long-lived excited electronic state. The most obvious candidate would perhaps be the metastable $4s3d\ ^1D_2$ state, but the photon energy at 397 nm is insufficient to ionise from this level (see Fig. 8c). Alternatively it is possible that the atoms are produced in bound Rydberg states, from which resonant transitions to some autoionising atomic states exist at 397 nm but not at 866 nm.

The outer electron in a high-lying Rydberg state atom can be viewed as a spectator that does not significantly interact with more tightly bound electrons. The transitions that are available to an atom in such a Rydberg state are therefore very similar to those available to the primary ion. The energy levels of the doubly-excited states can be approximated by superimposing the ionic energy level system onto each of the singly-excited Rydberg levels (see Fig. 8). It follows that regardless of the exact initial Rydberg state of the calcium

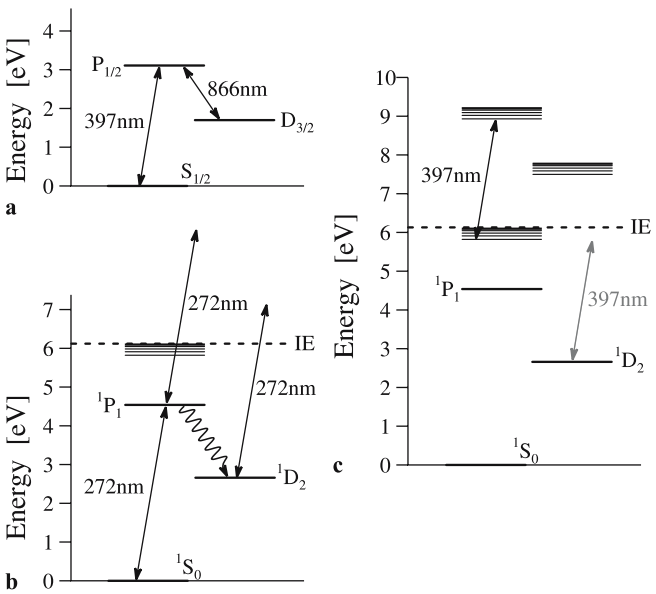

FIGURE 8 (**a**) Partial energy level diagram of Ca^+. (**b**) Partial energy level diagram of atomic calcium. (**c**) By superimposing the ionic energy levels onto each of the atomic Rydberg levels, we obtain approximate values for some of the doubly-excited autoionising states of atomic calcium

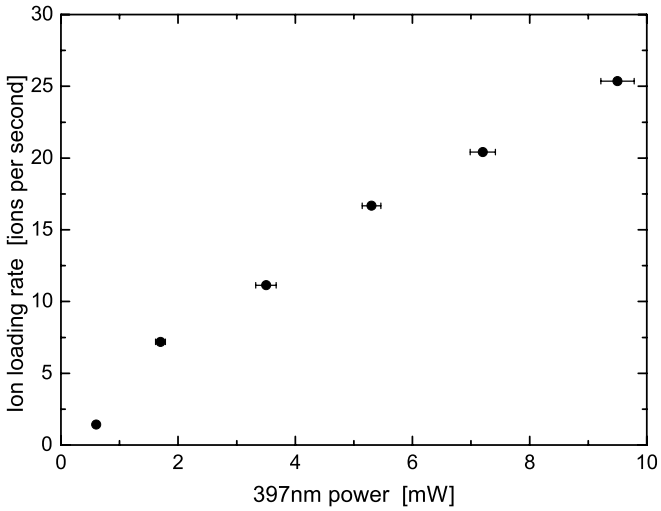

FIGURE 9 Ion loading rate as a function of 397 nm laser power. An initially linear relationship is observed, with possible saturation effects beginning to occur at higher powers. The ablation laser fluence used is 300 mJ/cm^2, with a repetition rate of 20 kHz

atoms there will always be a transition to an autoionising state close to the 397 nm ion cooling wavelength. The validity of this approximation is confirmed by detailed calculations and measurements of such an autoionising series in calcium [23].

We have studied the rate at which ions are loaded by this process as a function of 397 nm laser power. The results are presented in Fig. 9. An initially linear relationship is observed that shows some signs of saturation at higher powers.

Since the autoionising resonances are rather broad, this trap loading technique is not expected to be isotope selective and is therefore of limited use compared to resonant photoionisation of ground state calcium atoms. We note, however, that the same loading effect would be expected for any element that has a rapid Doppler cooling transition available to it in the ionic state. The technique may therefore be particularly useful for elements that only possess one isotope, such as beryllium, or where isotope selectivity is not required. The fraction of atoms produced in the Rydberg states, and hence the overall efficiency of this loading process, has yet to be determined.

6 Outlook

The general technique for ion trap loading presented here provides improved temporal control over the loading process, when compared to traditional methods. This may make it possible to reduce the overall amount of material passing through the trap, and hence to alleviate the problem of electrode contamination.

The technique can in principle be scaled down so that the target and laser delivery systems are integrated into microtrap structures. They would then form the basis of a 'loading zone', providing a stream of ions for a microtrap array. High-fluence laser ablation has previously been used for time-resolved studies of trapped, laser-cooled atoms [24]. The low-fluence ablation loading technique presented here may also be well suited to loading of the miniature atomic chip traps currently being developed [25].

Because the mean power dissipated in the ablation process is small, the loading technique presented here is compatible with traps operated at cryogenic temperatures. This feature may also be of interest to other parts of the ion and atom trapping community. Some species are not often trapped because very high temperatures are necessary to generate the required atomic beams. Chromium cells, for example, are often heated to almost 2000 K to achieve a sufficient vapour pressure for trapping [26, 27]. Maintaining a thermal source at such high temperatures makes it technically demanding to obtain low pressures in the vacuum chamber. By using a pulsed laser heating technique this problem might be alleviated.

Finally we note that the photoionisation of Rydberg state atoms using ion Doppler cooling transitions may be of benefit in ion trap experiments where isotope selectivity is not required, since it provides a simple route to some of the benefits of more complicated photoionisation schemes.

ACKNOWLEDGEMENTS The authors would like to thank Jacques Chevalier and Folmer Lyckegaard for technical assistance and numerous helpful discussions. This work is financially supported by the Carlsberg Foundation and by the EU under contract IST-517675-MICROTRAP.

REFERENCES

1 D. Leibfried, R. Blatt, C. Monroe, D. Wineland, Rev. Mod. Phys. **75**, 281 (2003)
2 H. Häffner, W. Hänsel, C.F. Roos, J. Benhelm, D. Chek-al-kar, M. Chwalla, T. Körber, U.D. Rapol, M. Riebe, P.O. Schmidt, C. Becher, O. Gühne, W. Dür, R. Blatt, Nature **438**, 643 (2005)
3 D. Leibfried, E. Knill, S. Seidelin, J. Britton, R.B. Blakestad, J. Chiaverini, D.B. Hume, W.M. Itano, J.D. Jost, C. Langer, R. Ozeri, R. Reichle, D.J. Wineland, Nature **438**, 639 (2005)
4 D. Kielpinski, C. Monroe, C. Wineland, Nature **417**, 709 (2002)
5 D.J. Wineland, D. Leibfried, M.D. Barrett, A. Ben-Kish, J.C. Bergquist, R.B. Blakestad, J.J. Bollinger, J. Britton, J. Chiaverini, B. Demarco, D. Hume, W.M. Itano, M. Jensen, J.D. Jost, E. Knill, J. Koelemeij, C. Langer, W. Oskay, R. Ozeri, R. Reichle, T. Rosenband, T. Schaetz, P.O. Schmidt, S. Seidelin, In: Proc. 17th Int. Conf. Laser Spect. (2005), pp. 393–402
6 D. Stick, W.K. Hensinger, S. Olmschenk, M.J. Madsen, K. Schwab, C. Monroe, Nature Phys. **2**, 36 (2006)
7 M. Brownnutt, G. Wilpers, R.C. Thompson, A.G. Sinclair, New J. Phys. **8**, 232 (2006)
8 L. Deslauriers, S. Olmschenk, D. Stick, W.K. Hensinger, J. Sterk, C. Monroe, Phys. Rev. Lett. **97**, 103 007 (2006)
9 R.G. DeVoe, C. Kurtsiefer, Phys. Rev. A **65**, 063 407 (2002)
10 N. Kjærgaard, L. Hornekær, A.M. Thommesen, Z. Videsen, M. Drewsen, Appl. Phys. B **71**, 207 (2000)
11 M. Cetina, A. Grier, J. Campbell, I. Chuang, V. Vuletić, arXiv:physics/0702025
12 N.S. Nogar, R.C. Estler, A.M. Miller, Anal. Chem. **57**, 2441 (1985)
13 M.N.R. Ashfold, F. Claeyssens, G.M. Fuge, S.J. Henley, Chem. Soc. Rev. **33**, 23 (2004)
14 C.R. Phipps (Ed.), *Laser Ablation and its Applications* (Springer, Heidelberg, 2007)
15 L. Balazs, R. Gijbels, A. Vertes, Anal. Chem. **63**, 314 (1991)
16 R. Kelly, A. Miotello, A. Mele, A. Giardini Guidoni, In: *Laser Ablation and Desorption*, ed. by J. Miller, R.F. Haglund (Academic Press, New York, 1998), pp. 225–289
17 A. Mortensen, J.J.T. Lindballe, I.S. Jensen, P. Staanum, D. Voigt, M. Drewsen, Phys. Rev. A **69**, 042 502 (2004)
18 A. Mortensen, PhD thesis, University of Aarhus, Institute for Physics and Astronomy (2005)
19 M. Drewsen, C. Brodersen, L. Hornekær, J.S. Hangst, Phys. Rev. Lett. **81**, 2878 (1998)
20 A. Mortensen, E. Nielsen, T. Matthey, M. Drewsen, Phys. Rev. Lett. **96**, 103 001 (2006)

21 D.N. Madsen, S. Balslev, M. Drewsen, N. Kjærgaard, Z. Videsen, J.W. Thomsen, J. Phys. B **33**, 4981 (2000)
22 P. Herskind, J. Lindballe, C. Clausen, J.L. Sørensen, M. Drewsen, Opt. Lett. **32**, 268 (2007)
23 A. Bolovinos, E. Luc-Koenig, S. Assimopoulos, A. Lyras, N.E. Karapanagioti, D. Charalambidis, M. Aymar, Z. Phys. D **38**, 265 (1996)
24 E.L. Raab, M. Prentiss, A. Cable, S. Chu, D.E. Pritchard, Phys. Rev. Lett. **59**, 2631 (1987)
25 J. Reichel, Appl. Phys. B **75**, 469 (2002)
26 C.C. Bradley, J.J. McClelland, W.R. Anderson, R.J. Celotta, Phys. Rev. A **61**, 053 407 (2000)
27 A. Griesmaier, J. Werner, S. Hensler, J. Stuhler, T. Pfau, Phys. Rev. Lett. **94**, 160 401 (2005)